

ARTICLES

Resonant inelastic x-ray scattering

P. M. Platzman and E. D. Isaacs

Bell Laboratories, Lucent Technologies, Murray Hill, New Jersey 07974

(Received 24 October 1997)

We analyze the physics of resonant inelastic x-ray scattering particularly from the $3d$ transition-metal series. We discuss what types and with what intensity we may expect to observe various final states, by considering an array of many particle dynamical effects. We conclude with the results of an experiment on $\text{NiS}_{1.5}\text{Se}_{0.5}$. [S0163-1829(98)01217-X]

INTRODUCTION

Inelastic x-ray scattering from electrons in condensed matter systems is a rapidly developing field which promises to give us detailed information about the excited states of these systems.¹ When the incident x-ray energy is far from any atomic absorption edges in the sample, inelastic scattering measures the dynamic structure factor of the electronic excitation spectrum. In some materials the low-lying electronic charge excitation spectrum consists of, for example, collective features such as plasmons, spin waves, excitons, and a single-particle-like continuum related to the band structure. The excitation energies of these spectral features and their momentum dependence can tell us a great deal about the role of electronic correlations, as well as the behavior of the material.

Because (10 KeV) hard x rays have a wave vector $q_1 = 2\pi/\lambda_1 \cong 5 \text{ \AA}^{-1}$, they are particularly well matched to studying the excitation spectrum over the entire Brillouin zone. However, because the scattering of x rays from electrons is weak, diffuse, and spread out in energy, and because the absolute energy resolution is so small ($\Delta\lambda_1/\lambda_1 \leq 10^{-4}$), most inelastic studies have been restricted to systems with low x-ray absorption in order to keep the scattering volume high.

Recently, it has been demonstrated that large enhancements in the scattering cross section can be achieved when the incident x-ray energy is tuned near to an atomic absorption edge of one of the atomic species in the sample.² Much as resonant enhancements have made it possible to study magnetic structure in a broad range of interesting condensed matter systems,³ resonance effects are now making it possible to study interesting electronic excitations previously inaccessible to inelastic x-ray scattering. In many electron systems interactions between electrons makes the possible excited states very interesting and the coupling to them extremely difficult to analyze even for the case of nonresonant scattering. On resonance, because of coupling to the deep atomic core hole, the analysis is even more difficult and possibly more interesting. Experiments with energy resolutions of 100 meV, which will soon be possible, should enable us to study relevant excited states as a function of momentum

transfer. They will compliment experiments such as resonant light scattering⁴ which are confined to nearly zero momentum and inelastic electron scattering⁵ which is confined to small momentum transfer and microscopically thin samples.

In this paper, we will focus on a discussion and analysis of the various physical phenomena which arise in such resonant scattering experiments particularly from the $3d$ transition-metal series. Since the resonant process is very local, exciting electron-hole pairs at a single atomic site, we will consider the role of the strong Coulomb interactions in these strongly correlated systems in accessing final excited states which, for example, involve a hole on one site and an electron on a neighboring site such as in a charge transfer or exciton.

We will not try to give a complete treatment of a particular sophisticated model problem since in a real solid there are too many diverse phenomena to consider. Instead, we will emphasize the order of magnitude of the various effects and stay away from detailed calculations. We will also address the important issue of momentum transfer and conservation in the context of the resonant inelastic cross section.

We will then present the results of an experiment in the classic Mott-Hubbard system $\text{NiS}_{1.5}\text{Se}_{0.5}$ (Ref. 6) which undergoes a metal-insulator transition at $T_c = 80 \text{ K}$ in our sample.⁷ Our discussion will center on the momentum dependence of the position and intensity of a well-defined feature in the inelastic scattering spectra with an energy loss of about 5.5 eV in the insulating phase. We associate this feature with the creation of an exciton involving the excitation of an electron from a sulfur state to the upper Hubbard $3d$ band associated with the nickel. The momentum dependence of this feature clearly demonstrates that the momentum transferred to the system is carried, at least in part, by the final excited state as it is in the simpler nonresonant excitation processes.

In a typical scattering experiment, an x ray of energy ω_1 , polarization ε_1 , and momentum \mathbf{q}_1 ($\hbar = 1$) scatters weakly from the electronic system in an initial (ground) many-body state $|i\rangle$ to a final state $(\omega_2, \varepsilon_2, \mathbf{q}_2)$. This leaves the system in an electronically excited state $|f\rangle$ with momentum $\mathbf{q} \equiv \mathbf{q}_2 - \mathbf{q}_1$ and energy $\omega \equiv \omega_1 - \omega_2$. In the nonrelativistic limit ($\omega_1 \ll mc^2 = 5 \times 10^5 \text{ eV}$), the matrix element for scattering,

to second order in the electromagnetic field is given by

$$M = \frac{e^2}{mc^2} \left[\langle f | \boldsymbol{\varepsilon}_2 \cdot \boldsymbol{\varepsilon}_1 \rho_{\mathbf{q}} | i \rangle + \left(\frac{1}{m} \right) \left\{ \frac{\langle f | \mathbf{p}_{\mathbf{q}_2} \cdot \boldsymbol{\varepsilon}_2 | n \rangle \langle n | \mathbf{p}_{\mathbf{q}_1} \cdot \boldsymbol{\varepsilon}_1 | i \rangle}{E_n - E_i - \omega_1 + i\delta} \right. \right. \\ \left. \left. + \frac{\langle f | \mathbf{p}_{\mathbf{q}_1} \cdot \boldsymbol{\varepsilon}_1 | n \rangle \langle n | \mathbf{p}_{\mathbf{q}_2} \cdot \boldsymbol{\varepsilon}_2 | i \rangle}{E_n - E_i + \omega_2} \right\} \right], \quad (1)$$

here $\rho_{\mathbf{q}} \equiv \sum_j e^{i\mathbf{q} \cdot \mathbf{r}}$ is the density operator, $\mathbf{p}_{\mathbf{q}} \equiv \sum_j \mathbf{p}_j e^{i\mathbf{q} \cdot \mathbf{r}}$ is the momentum operator. The energies $E_i(E_n)$ are the energy of the ground (intermediate) state of the interacting many-body system with correlated wave functions ($|i\rangle, |n\rangle$).

When ω_1 is not near the binding energy of an atomic core state, Eq. (1) is dominated by the first term on the right-hand side and the scattering cross section at $T=0$ can be written as⁸

$$\frac{d\sigma}{d\omega d\Omega} = (\varepsilon_{1\alpha} \varepsilon_{2\beta} \delta_{\alpha\beta})^2 \left(\frac{e^2}{mc^2} \right)^2 \\ \times \sum_f |\langle f | \rho_{\mathbf{q}} | i \rangle|^2 \delta(E_f - E_i - \omega), \quad (2)$$

which is only a function of \mathbf{q} and ω . Since $(e^2/mc^2)^2 \cong 10^{-26} \text{ cm}^2$ is small and since the number of interesting (valence) electrons, $n \cong 10^{22} \text{ cm}^{-3}$, the total scattering is rather weak. This is why, as mentioned above, even with the best synchrotron sources, inelastic scattering rates are low and it is thus only possible to do nonresonant inelastic scattering experiments on materials with small absorption.

When the incident x-ray energy is tuned near to the binding energy of a deep core level of an atom in the system, the second term in Eq. (1) dominates the cross section. In this case the energy denominator can vanish and the cross section can become large. However, the cross section also becomes more complicated than Eq. (2), in that the nature of the coupling to the excited state $|f\rangle$ depends on the presence of the intermediate state $|n\rangle$ which contains an almost real, strongly perturbing core hole. Nevertheless the cross section can still be written as in Eq. (2). It is

$$\frac{d\sigma}{d\omega d\Omega} = (\varepsilon_{1\alpha} \varepsilon_{2\beta})^2 \left(\frac{e^2}{mc^2} \right)^2 \sum |\langle f | O_{\mathbf{q}}^{\alpha\beta} | i \rangle|^2 \\ \times \delta(E_f - E_i - \omega). \quad (3)$$

The finite \mathbf{q} resonant Raman operator $\mathbf{O}_{\mathbf{q}}$ conserves momentum and gets large when ω_1 is near an absorption edge. In principle $\mathbf{O}_{\mathbf{q}}$ is a function of ω_1 , \mathbf{q}_1 , \mathbf{q}_2 , $\boldsymbol{\varepsilon}_1$, $\boldsymbol{\varepsilon}_2$. The tensor character of $O_{\mathbf{q}}^{\alpha\beta}$ arises from the momentum operator in the matrix elements. As we shall see, this implies that we can couple to transverse and spin excitations as well as longitudinal excitations.

No one has successfully given a complete many-body description of the operator $O_{\mathbf{q}}^{\alpha\beta}$.⁹ However, making the assumption that the intermediate state energy denominator can be replaced by some average energy allows one to sum over intermediate states and reduce the problem to the calculation of an autocorrelation function, as in the nonresonant case, of a simple operator such as $\rho_{\mathbf{q}}$.¹⁰ Such approaches are not generally valid and we will discuss their limitations later in the article.

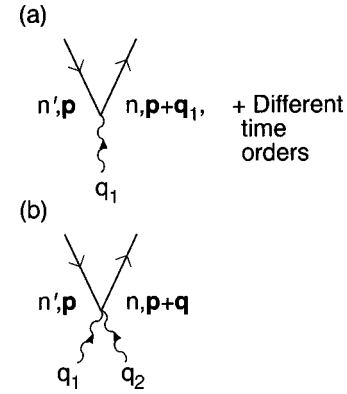


FIG. 1. Perturbation theory diagrams for the interaction of x-ray photons of momentum $\mathbf{q}_1, \mathbf{q}_2$ with band electrons.

In order to better understand many of the interesting aspects of Eq. (3), we now turn to a discussion of some of the physics contained in the resonance process.

THEORETICAL CONSIDERATIONS

To establish a framework for discussing the various physical processes involved and to include Coulomb interactions we choose to represent the scattering processes by a set of time ordered Feynman diagrams which are nothing more than pictorial representations of the various terms in the perturbation expansion of the full many-body problem.¹¹ The perturbation terms include the coupling of the x rays to the system, which is weak, as well as the coupling of the electrons to each other and to the nuclei via their Coulomb interactions, which is not. Since the various Coulomb couplings are not weak we will often have to sum many terms in the perturbation series in the Coulomb interactions between electrons to display a given effect. In many cases this can be easily represented graphically.

The x rays primarily interact with the system to make electron hole pairs. In Fig. 1(a), an x ray of momentum \mathbf{q}_1 (wiggly line) is annihilated and an electron is excited from a filled band state n' to an empty band state n . Energy is not conserved if the electron-hole pair is an intermediate state, however, crystal momentum, i.e., momentum plus or minus some reciprocal lattice vector \mathbf{K}_n is conserved at each vertex. The electrons and holes (empty states) propagating in the valence bands of the material are represented by solid lines. Those lines going up (forward in time) are electrons while those going down (backward in time) are holes. Since the hole in one of the inner shells (for example a hole in the K shell) plays a unique role, we will designate it by a double solid line, and label it with a \mathbf{c} . The fact that the solid lines represents a band state means that we have already implicitly included all the multiple elastic scattering of the electrons from the nuclei and from the mean (in the local density sense) charge of the other electrons (exchange included) in the details of these states. The scattering due to the $\rho_{\mathbf{q}}$ term in Eq. (1), can also create an electron-hole pair at a single vertex where the initial photon is destroyed and the final one created [see Fig. 1(b)].

The photons can also couple to phonons by two quite distinct mechanisms. The first and most commonly accepted way is to first excite an electron hole pair and then have

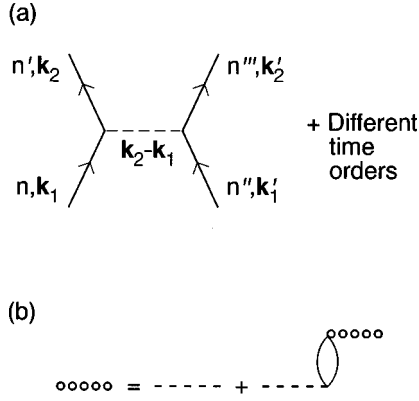


FIG. 2. (a) Electron Coulomb scattering diagram; (b) screening of the bare Coulomb interaction [dotted line in (a)] by valence band electron hole pairs.

either the electron or hole scatter quasielastically from the nucleus or equivalently the deeply bound electrons creating a phonon and leaving an electron hole pair. The second is to couple directly to the center of mass motion as discussed by Platzman, Tzoar,¹⁰ and Sette.¹² In either case, processes involving phonons lead to momentum nonconserving effects. As far as the electronic excitations are concerned, such effects will lead in many cases to a broad featureless background which can often be ignored. In any event they will not be of primary concern to us here, although we will discuss some aspects of them.

In addition to coupling to the electromagnetic (EM) field the electrons can couple to each other by direct Coulomb interactions (dashed line), see Fig. 2(a). Each dashed line corresponds to a matrix element $\phi_n(\mathbf{k}) = [4\pi e^2 / (\mathbf{k} + \mathbf{K}_n)^2] F(\mathbf{K}_n)$, where $\mathbf{k} = \mathbf{k}_1 - \mathbf{k}_2$. The form factor $F(\mathbf{K}_n)$ for the Coulomb matrix element for different reciprocal lattice vectors \mathbf{K}_n depends on the Fourier transform of the Bloch parts of the scattering electrons wave functions. For the electron gas, i.e., electrons in a uniform positive background, $F(\mathbf{K}_n) = \delta_{0, \mathbf{K}_n}$.

In order to include cooperative effects in a mean field random-phase approximation (RPA) sense, e.g., plasmons for free electronlike metals, we generally screen $\phi_n(\mathbf{k})$ by the dielectric function. More precisely we replace $\phi_n(\mathbf{k})$ by $\phi_n(\mathbf{k})/\epsilon(\mathbf{k}, \omega)$. The replacement is equivalent to changing the bare (dashed) Coulomb line in Fig. 2(a) into a dressed (braided) Coulomb line pictorially represented by the infinite set of diagrams shown in Fig. 2(b). When there are significant band structure effects $\epsilon(\mathbf{k}, \omega)$ is a tensor, e.g., $\epsilon_{n, n'}(\mathbf{k}, \omega)$ with (n, n') band indices) and the situation is more complicated, i.e., the various interband terms represented by $\epsilon_{n, n'}(\mathbf{k}, \omega)$ with $n \neq n'$ must be included.^{7,13}

Near resonance and in the *absence* of any interaction effects the time ordered diagram which dominates the resonance cross section is shown in Fig. 3. This process leads to a matrix element ($\delta \rightarrow 0$),

$$A_0 = \frac{\langle 1s | \mathbf{p}_2 \cdot \boldsymbol{\epsilon}_2 e^{i\mathbf{q}_2 \cdot \mathbf{r}_2} | v, \mathbf{p} - \mathbf{q}_2 \rangle \langle v, \mathbf{p} + \mathbf{q}_1 | \mathbf{p}_1 \cdot \boldsymbol{\epsilon}_1 e^{i\mathbf{q}_1 \cdot \mathbf{r}_1} | 1s \rangle}{m(E_{v, \mathbf{p} + \mathbf{q}_1} - E_{1s} - \omega_1 + i\delta)}. \quad (4)$$

Here, A_0 is dimensionless and its contribution to the cross section is given relative to the leading term in Eq. (1) which

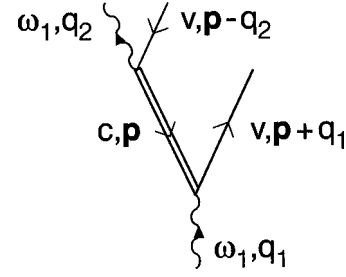


FIG. 3. The lowest order noninteracting matrix element for resonant inelastic x-ray scattering.

is of order one and $|v, \mathbf{p}\rangle$ refers to some good one electron approximation to a valence band wave function with a crystal momentum \mathbf{p} .

In the absence of Coulombic effects the energy denominator in Eq. (4) has a real singularity. The singularity means that the second order matrix element describing scattering, has become a single photon absorption process, followed by a single photon emission. The divergence is nothing more than a statement of the fact that the time available for absorption under steady state conditions is infinite.² Of course in a real system with Coulomb interactions the core hole decays predominantly nonradiatively with a lifetime Γ^{-1} . To take this into account it is acceptable to replace δ by Γ . For scattering near a K edge Γ comes primarily from the Auger decay of the $1s$ core hole to a $2s$, $2p$ hole, i.e., it is nonradiative. In transition metals such as Ni and Cu Γ is a few eV and the particle hole pairs which are excited have energies $\Delta E_{\text{Aug}} \cong E_{1s} - E_{2p}$ which are nearly a kilovolt.

When the incident and emitted photons are much closer in energy than ΔE_{Aug} , the lifetime Γ is a good way of phenomenologically including a host of many-body effects that do not interest us. It correctly limits the size of the resonant enhancement, and gives us a rough estimate of the amount of x rays which are scattered and which still conserve energy and momentum. In addition it tells us correctly that a range of states off the energy shell of the order of Γ fix the resonant matrix element.

At the intermediate state energies for hard x rays condensed matter systems have a continuum of energies. Thus no single intermediate state dominates the scattering process and most of the intermediate states which contribute are off the energy shell by an amount Γ . *However, independent of the many electron origins of Γ , it is always true that if there is one photon in and one photon out the many-body system is left in an excited state with momentum \mathbf{q} and energy ω .* The lifetime of the core hole will *not* contribute to the width of features in the spectrum. For example, in a semiconductor the band edge will be sharp, i.e., spectrometer resolution limited. An excitonic feature will be there with a width determined by its decay. Moreover, it should be possible to observe sharp many-body features, provided they have large enough matrix elements. In general though, there are almost always a rather broad continuum of states even at excitation energies of 10 eV and the presence of a peak implies something more subtle about the many electron system.

The most obvious and common examples are a plasmon or a spin wave collective state. For the case of a simple metal

such as aluminum we will predict that the plasmon excitation will be present at low \mathbf{q} and that it will disperse exactly as in the nonresonant case.

Now that we have digressed a bit, discussing at least qualitatively how some Coulomb effects modify our interpretation of Eq. (4) even in the noninteracting approximation, let's go back to Eq. (4) for some more discussion of the physics. The matrix elements in Eq. (4) are clearly very local. They involve matrix elements of the single particle momentum operator \mathbf{p} sandwiched between a K shell ($1s$) core wave function which is very confined compared to the incoming x rays wavelength, and a partially filled valence band (VB) electronic wave function which is spread out. This means we need the atomic part of the VB wave function. The evaluation of such matrix elements has been carried out for the L shell ($2p$) core wave function in rare-earth compounds by Carra *et al.*⁹ and at the soft x-ray edges such as in graphite¹⁰ and CaF_2 .¹⁴

When we excite near the K edge of a transition metal ion the matrix elements are even more local. However, the best one electron estimate of the local part of the wave function involves one additional bit of physical intuition. Suppose that the valence state of nickel in our transition-metal compound is approximately Ni^{++} , i.e., it has a $3d^8$ configuration. The dipole allowed transition to the first empty state, which is a valence band state in the solid, is to a VB state, which has at small distance from the Ni^{++} $4p$ atomic character. However, because the transition is so high in energy ($\Delta E \cong 9$ keV) it is sudden. Since the core hole is slow to relax it is much better to think of the $4p$ atomic wave function as the $4p$ in a Cu^{++} with $(3d^8, 4p)$ configuration, i.e., the $Z+1$ atom describes the frozen hole in the atom with charge Z .

We have used a local density approximation (LDA) atom program¹⁵ to evaluate matrix elements relevant to Ni ($\text{S}_{1.5}/\text{Se}_{0.5}$). For Ni^{++} in the frozen hole approximations as discussed above the important matrix elements are $\langle 4p|r|1s \rangle \cong 0.6$ a.u. and $\langle 3d|r(\partial/\partial r)|1s \rangle |1s \rangle \cong 0.01$ a.u. Using these matrix elements, a $\Gamma \cong 2$ eV and a $q_1 = 2$ a.u., we find that the resonant cross section is roughly a factor of 100 larger than its nonresonant counterpart.

While the matrix elements are local, the coherent effect of adding up many matrix elements involving tightly bound electrons at different lattice sites should for a noninteracting system lead to overall crystal momentum conservation.⁸ However, in our case, in the presence of interaction effects momentum conservation for a K shell hole intermediate state is a bit subtle and interesting. Since Γ the Auger width is $\gg \Delta E_{1s}$, where ΔE_{1s} is the band width of the $1s$ core hole, the deep core hole has no idea it is in a crystal lattice. Different matrix elements from different lattice sites will not interfere. Instead the initial x-ray photon gives its momentum to the outgoing electron and to a recoiling transition metal ion. Since $\Gamma \gg \omega_D$, the lattice Debye frequency, the momentum given the single transition metal ion is returned to the electronic system when the final x-ray photon is emitted. The emission of a real phonon in this process leads to momentum breaking. The size of such a momentum breaking process caused by the intermediate state recoil will be small, i.e., of order ω_D/Γ relative to the momentum conserving piece since most intermediate states are off the energy shell by an amount Γ .

The noninteracting expression forms the basis for all the early discussions of resonant x-ray scattering. Carlisle *et al.*¹⁶ have applied a one electron single particle description to a set of experiments in graphite. They were able to show a correlation between the noninteracting picture and the band structure of Graphite. Veenendaal *et al.*⁹ developed a theory of resonant x-ray scattering for the rare earths which was one electron in character and made the additional assumption that the energy E_n in the denominator could be replaced by some average or typical \bar{E}_n . This assumption is in their case not quantitatively accurate because Γ is smaller than separation between various bands. For example, in Ni^{++} the dominant transition at resonance is to the $4p$ level. The $5p$ levels, etc., are roughly 10 V away, so that with $\Gamma \cong 2$ eV these transitions are down by almost one order of magnitude from the energy denominator alone and another factor of 2 or so from the matrix element. Replacing the denominator by an average \bar{E}_n means we take (in an atomic picture) all p levels $4p$, $5p$, continuum, etc., weighted only by their matrix element. A better approximation (for Γ small) is to take one state, i.e., in our case only $4p$. Nevertheless, in Ref. 9 they do show that their theoretical noninteracting average energy approximation does reproduce some symmetry features of the experiments by Hamalainen *et al.*,¹² who probed excitations near the Dysprosium L_3 edge with inelastic x-ray scattering.

Despite all the complications associated with explicitly evaluating Eq. (3) it is quite clear from Fig. (3) that this resonant coupling leads to a *single* electron-hole pair with a particular weighting which depends primarily on the energy denominator in the intermediate state, and which conserves crystal momentum. Since crystal momentum is conserved, this resonant process is a bit similar to having the operator $\rho_{\mathbf{q}}$ acting on the ground state just as in the nonresonant case. There is, of course, an enhanced magnitude. However, there is an important distinction which is related to the general properties of the resonant operator. For the first term in Eq. (1) the density operator is precisely $\rho_{\mathbf{q}}$, where $\rho_{\mathbf{q}} = \sum_{\mathbf{p}, n, n'} a_{\mathbf{p}+\mathbf{q}, n'}^+ a_{\mathbf{p}, n}$ creates an electron at momentum $\mathbf{p}+\mathbf{q}$ and a hole with momentum \mathbf{p} . In contrast, for the resonant process the $O_{\mathbf{q}}^{\alpha\beta}$ in Eq. (3) may be written schematically,

$$O_{\mathbf{q}}^{\alpha\beta} = \sum_{\mathbf{p}, n, n'} A_0^{\alpha\beta}(\mathbf{p}, \mathbf{q}_1, \omega_1, \mathbf{q}_2, \omega_2) a_{\mathbf{p}+\mathbf{q}, n'}^+ a_{\mathbf{p}, n}, \quad (5)$$

where the subscript 0 on A means no Coulomb interaction.

To next order (first) in the Coulomb interactions among the electrons and between the virtual core hole and the electrons we must consider the scattering processes depicted by the diagrams shown in Fig. 4.¹⁰ While it is possible to evaluate such terms in some detail it is really unnecessary, since we really want to know their approximate size and possibly what new kinds of final excited states can be reached. Ultimately, we might also want to consider how the details of the matrix element might influence the line shape.

Because the perturbation diagrams in Fig. 4 all have one resonant denominator and one extra Coulomb interaction they will generally be of order $\langle \phi \rangle / \Gamma \cong 1$ relative to the zeroth order diagram shown in Fig. 3. Diagrams I–IV in Fig. 4 (as for Fig. 3) lead to a single pair final state. Insofar as the pair is on the same transition metal site, this process is simply a modification of the amplitude A_0 Eq. (5). However, often the

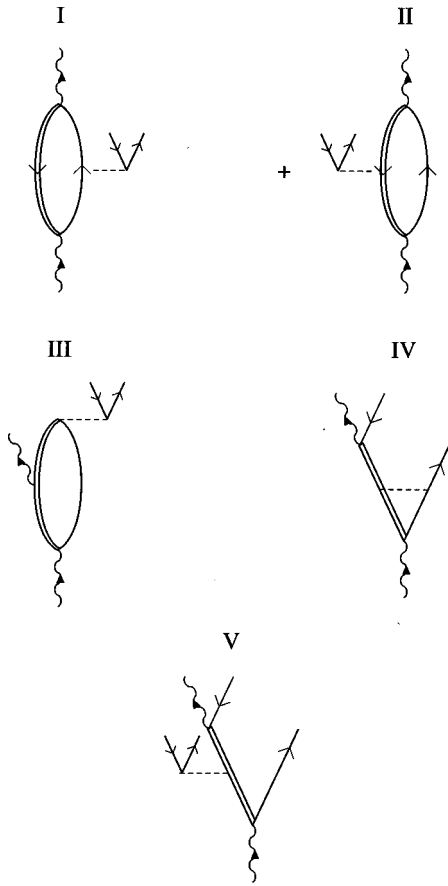


FIG. 4. The first order Coulomb interaction (horizontal dotted line) corrections to resonant inelastic x-ray scattering.

important low-lying excitations involve the excitation of an electron from the cation (e.g., oxygen) to the anion (e.g., copper) on a neighboring lattice site, a so-called charge transfer excitation. To zeroth order (Fig. 3) in the Coulomb interaction such excitations are very weak since there is little overlap in the wave function, for example, of an electron on a neighboring oxygen with the localized core states of a Ni^{++} to create such an extended excitation. However, in diagrams I–III in Fig. 4 such excitations are present, i.e., the Auger-like pair produced by the dashed Coulomb line can be on different sites because of the substantial overlap of the outer electrons at different sites.

Diagrams I and II are shakeup process produced by the intermediate state $4p$ electron $1s$ hole. The pair produced is in the final state so the Coulomb matrix element contains a $1/q^2$ factor. In addition the final vertex is again dipole allowed, i.e., the $4p$ electron falls back into the $1s$ hole. Diagram III for Ni^{++} the initial photon resonantly creates the $4p$ state and a $1s$ hole. The final photon is emitted at the next vertex and the $1s$ core hole changes into a (dipole allowed) $2p$ core hole. The matrix element is dipole allowed and about one to two orders of magnitude larger than the $4p$ matrix element which dominates diagrams II and III. Nevertheless, it has an intermediate state which is off the energy shell by the binding of the $2p$ (1 keV) which means that it is suppressed by roughly $\langle \phi \rangle / (E_{2p} - E_{1s}) \cong 10^{-2}$. The final vertex is Coulomb-like, i.e., the $2p$ hole annihilates creating the particle hole pair in the valence band. The matrix element

has a $1/q^2$ piece and is of order $\langle \phi \rangle / \Gamma \cong 1$ as discussed earlier. So we conclude that diagrams I–III in Fig. 4 are roughly equal and an order of magnitude larger than the noninteracting expression Eq. (4) in most transition-metal compounds. In addition they can lead to charge transfer excitons. In the charge transfer case the Coulomb matrix element has an overlap factor in it which probably makes the matrix element somewhat smaller than the noninteracting overall one (see Fig. 3).

Diagram III (Fig. 4) also describes the coupling between a virtual absorption process and a true nonresonant Raman process. As we have already discussed the off energy shell electron-hole pair present just before the Coulomb interaction could be the pair produced in a “real” luminescence process. Since for our final state it is virtual, i.e., off the energy shell, it lives a short time decaying into the Raman-like final state by means of a Coulomb coupling. If the real final state is characterized by a sharp peak, e.g., the pair is an exciton or a plasmon as discussed below, then this type of lowest order virtual coupling to the continuum of luminescence states can change the line shape leading to a so-called Fano line shape.¹⁷ If the final state is a continuum, then the line shape will also be distorted in a different way which we discuss in some detail.¹⁸

Diagram IV is an interesting one. The dipole matrix element at the first vertex produces a p -like electron. Since for the transition metal sulfides and oxides this state is about 15 eV above the occupied $3d$ states,⁷ it is quite extended. This p state can scatter from the core hole falling easily into a $3d$ state on a neighboring transition-metal site. The annihilation of the occupied $3d$ implies we have transferred a $3d$ electron from one site to another. However, it is important to note that this diagram does not have the $1/q^2$ dependence of the other three diagrams, and it is reduced by one order of magnitude by the quadrupole matrix element involved in the final $d \rightarrow s$ transition, but there is no overlap as in the charge transfer case.

Diagram V in Fig. 4, which is also lowest order in the Coulomb interaction, leads directly to two pair final states, i.e., it breaks momentum conservation and it behaves a bit like¹⁹

$$\sum_{k'} \rho_{k'} \rho_{-k'+q} |i\rangle. \quad (6)$$

Of course the coefficient weighting the two pair shakeup operator is not simply unity but depends in detail as in Eq. (4), on the initial photon energy as well as the exact single particle states which are excited in the final state. Such a two pair process breaks the single pair momentum conservation and allows us to observe states which because of some selection rule are almost orthogonal to $\rho_{\mathbf{q}} |i\rangle$. It is well known by now that resonant Raman light scattering spectra from carriers in the fractional quantum Hall regime are dominated by this kind of two pair shakeup process.¹⁹ More precisely, such experiments rather conclusively show the presence of a two magneto-Roton bound state. The sharp, feature is very specific to the quantum Hall systems but the finite intensity near $q = 0 \text{ \AA}^{-1}$ (only regime accessible with light) is related to Fig. 4, diagram V. The lowest order two pair shakeup coupling mechanism is the same in both systems.

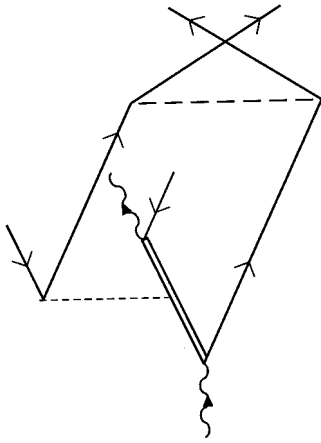


FIG. 5. A schematic picture of a possible two magnon inelastic x-ray scattering process.

For strongly correlated Mott-Hubbard insulators such a two pair processes could enable us to observe a two-magnon process.⁵ More specifically two electrons are excited on neighboring sites, with at least one in an empty p state. Then in perturbation theory a simple Coulomb exchange process which has quite a large matrix element allows the p electron assumed to be on site 1 and have for example spin up to wind up in a d -like state on site 2 while the d electron on site 2 with spin down winds up in a d state on site 1 (see Fig. 5). The two holes left in the figure reflect the fact that we have annihilated the electrons which were occupying the orbital originally and replaced them with the electrons of opposite spin. The exchange of the two spins in the antiferromagnetic Mott-Hubbard insulator is a two magnon process whose detailed shape depends on the initial x-ray energy and on the momentum transferred. In the case under discussion it will also depend on the initial frequency ω_1 . Such x-ray experiments should clearly display the two magnon piece in antiferromagnetically ordered insulators.

Our discussion has been based on simple arguments about the nature of a few low order terms in a perturbation expansion. Such arguments make it very clear that an important aspect of the resonant x-ray scattering process, is that because the excited p state is so high in energy, a resonant scattering in transition metal oxides can easily access *all* the electronic excited states including those which involve near or next-neighbor overlap and those which have magnetic character. Our discussion emphasizes the fact that simple energy conservation implies that the nonradiative intermediate state lifetime Γ^{-1} *does not* limit the resolution but does limit the size of enhancement which is still very significant.

In order to include many important higher order Coulomb effects as discussed we simply screen the bare dashed Coulomb interaction by the dielectric constant (tensor) $\varepsilon_{n,n'}(\mathbf{k}, \omega)$, which amounts to summing bubbles as in Fig. 3. For the resonant single pair scattering this implies that the amplitude is given (neglecting local field effects) schematically by the operator

$$O_{1c} = \left[A_0 + \frac{\phi_q \Lambda}{\varepsilon_0(\mathbf{q}, \omega)} \right] a_{\mathbf{p}+\mathbf{q}}^+ a_{\mathbf{q}}. \quad (7)$$

The vertex $\phi_q \Lambda$ is shorthand for the sum of diagrams I–IV in Fig. 4, where the final state is now on the same transition-metal site. The nonresonant process has a similar structure except there $A_0 = 1$ and $\Lambda = Q_0(\mathbf{q}, \omega)$, where

$$\varepsilon_0(q, \omega) = 1 - \phi_q Q_0(q, \omega) \quad (8)$$

and ε_0 is the mean field Lindhard function. Screening the Coulomb interaction this way sums all of the terms with powers of $1/q^2$, i.e., it gives us a physically meaningful result at low momentum transfers.

The form of Eq. (7) tells us that in resonant scattering, as in nonresonant, there will be a peak at a zero of $\varepsilon_0(\mathbf{q}, \omega)$, i.e., a collective plasmon mode in simple metal appears with a modified strength. Since such a mode in any real material has a width, the complicated form of the vertex distorts the shape. In addition since A_0 and $\Lambda \neq 1$, as in the nonresonant case, there will be incomplete screening of the single particle continuum. In a simple metal, at low q all the weight in the spectrum is in the plasmon.⁷ For resonant scattering a finite fraction of the scattering will be in the particle hole continuum. In a real sense the resonant process couples to transverse currents which are unscreened, and the weight in the low-energy particle hole continuum is for simple metals roughly proportional to

$$W = \left| \frac{\Lambda - Q_0(q, \omega)}{Q_0(q, \omega)} \right|^2. \quad (9)$$

In many instances $|\Lambda| \gg |Q_0|$ and all of the weight is in the single particle continuum even at low momentum transfers.

In transition-metal complexes such as $\text{NiS}_{1.5}\text{Se}_{0.5}$ the screening problem is obviously much more complex. There is no well defined zero of the real part $\varepsilon(\mathbf{q}, \omega)$ primarily because interband transitions are strong and overlap with any zero of the real part. In such materials ε will partially screen the effects of the $1/q^2$ matrix element and ultimately soften the dependence of the cross section of \mathbf{q} , particularly at modest ($q \approx 1$ a.u.) momentum transfers.

RESONANT INELASTIC X-RAY SCATTERING IN $\text{Ni}(\text{S}/\text{Se})_2$

As we have tried to make clear, the processes leading to resonant inelastic x-ray scattering are somewhat more complex and interesting than the nonresonant one. A complete theoretical understanding is at best very difficult. Therefore, in this section we will attempt to shed some light on these resonant processes by describing them in the context of a recent experimental result.

We will focus on inelastic scattering measurements in the classic Mott-Hubbard system $\text{Ni}(\text{S}/\text{Se})_2$. NiS_2 is an insulator and NiSe_2 is a metal. The ternary alloy $\text{Ni}(\text{S}_{1-x}\text{Se}_x)_2$ has a phase diagram which includes an insulator-metal transition and antiferromagnetism. For instance, the alloy $\text{NiS}_{1.5}\text{Se}_{0.5}$ is a nonmagnetic insulator at room temperature and becomes metallic upon cooling below $T_c = 85$ K. The main valence band features are the $\text{Ni}(3d)$ electrons and the S/Se $3p$ states. The highest occupied state, according to LDA,²⁰ is a half-filled $\text{Ni } e_g$ band ($3d$) which via strong Coulomb correlations splits into an upper and lower Hubbard band with a gap of about $U \approx 5$ eV.²¹ The antibonding $\text{S } pp\pi^*$, between

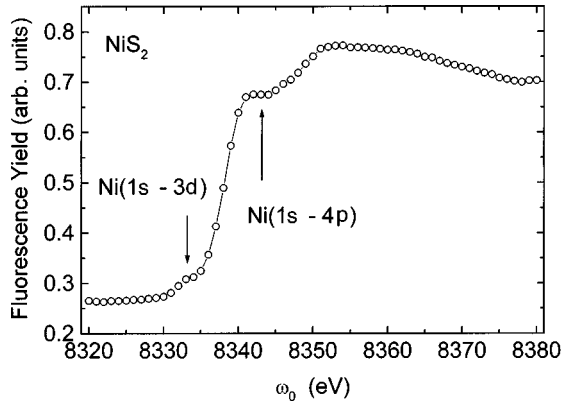


FIG. 6. The absorption profile of x rays near the K edge of nickel in NiS_2 .

the upper and lower Hubbard bands, then becomes the highest occupied state.²² In this picture, NiS_2 is a charge transfer insulator with a gap of about 2 eV (Refs. 14 and 18) between the S $pp\pi^*$ and the upper Hubbard band. In the inelastic x-ray scattering measurements of Ref. 23, with an energy resolution 1 eV, we focus on electronic excitations among these valence states at intermediate energy transfers.²³

We start our discussion of experimental results with a description of the x-ray absorption, which is directly related to the first vertex in Fig. 3. All of the data we show were measured at the dedicated inelastic scattering beamline X21 at the National Synchrotron Light Source. Figure 6 shows the absorption profile near the Ni $K\alpha$ emission lines (7.478 and 7.461 keV) with an energy dispersive detector. As discussed above, the feature at 8.344 keV can be thought of as a dipole transition from a $\text{Ni}^{++}|1s\rangle$ core state to an unoccupied $\text{Cu}^{++}(Z+1)|4p\rangle$ band state. We can also see the weaker feature at 8.3325 keV, which can be ascribed to the quadrupolar $|1s\rangle$ to $|3d\rangle$ transition. The ratio in intensities of these two features of roughly a factor of 50 is consistent with our LDA estimate of the matrix elements. The resonance enhancement occurs at the 8.344 keV feature.

Figure 7 shows inelastic scattering of x rays in $\text{NiS}_{1.5}\text{Se}_{0.5}$ with the incident energy tuned to the peak of the absorption at 8.344 keV. The energy of the scattered photons was analyzed with a spherically bent (1 m radius) Si(553) crystal placed 1 m from the sample. Since the intrinsic resolution of the Si(553) is approximately 50 meV, the energy resolution of 1 eV was determined by a combination of the incident energy resolution [0.7 eV at 8.4 keV as determined by the Si(220)] monochromator and the size of the x-ray spot on the sample. The very bright peak at zero energy loss ($\Delta E = E - E_0 = 0$) is quasielastic scattering from the sample, which includes contributions from phonons whose energies (<100 meV) are too small to resolve.⁷ The remaining features are resonant inelastic x-ray scattering.

The rather broad peak centered at an energy loss of 15 eV we ascribe to the excitation of a $3d$ electron on the nickel to the empty $4p$ state. This broad peak has only a weak q dependence which would indicate that it is dominated by the direct process (Fig. 3). In addition it is so broad that it is difficult to determine how it moves with ω_1 .

The spectrum below the energy loss is more interesting.

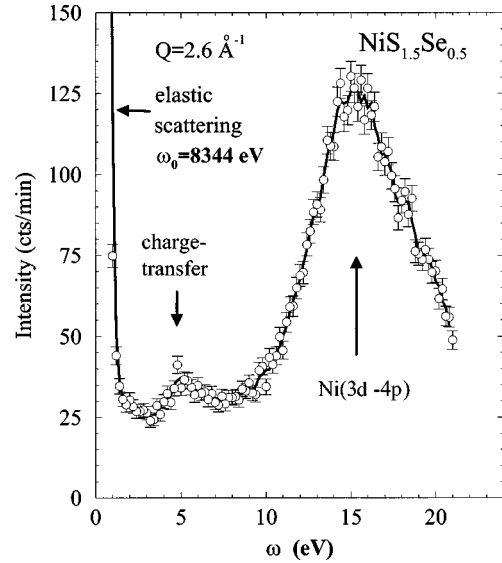


FIG. 7. The resonant inelastic spectrum of $\text{NiS}_{1.5}\text{Se}_{0.5}$ for $\omega_1 = 8344$ eV.

The well defined feature at 5 eV tracks the incident energy, i.e., it has a roughly constant energy loss. The peak intensity also decreases rapidly as the incident energy is varied from 8.344 keV and cannot be detected above background when ω_1 is ± 5 from 8.344 keV.

Figure 8 shows the spectrum taken with an energy of 8.344 keV plotted versus ΔE for four different momentum transfers. The data is shown out to $\Delta E = 15$ eV in order to emphasize the peak at 5 eV. Here, the quasielastic scattering is centered at $\Delta E = 0$ eV and the large positive slope at the higher energy-loss is the tail of the $3d$ - $4p$ excitation described in the previous paragraph (see Fig 7). In addition to the peak at 5 eV we also note a weaker peak at 9.5 eV. The momentum transfer dependence of the spectra in Fig. 8 is seen as both a variation in the position and intensity of the peak near 5 eV. At $q = 1.5 \text{ \AA}^{-1}$ the peak position is $\Delta E = 5.5$ eV and at $q = 4.2 \text{ \AA}^{-1}$ the peak position has decreased to $\Delta E = 5$ eV or by about one-half a linewidth. Perhaps more

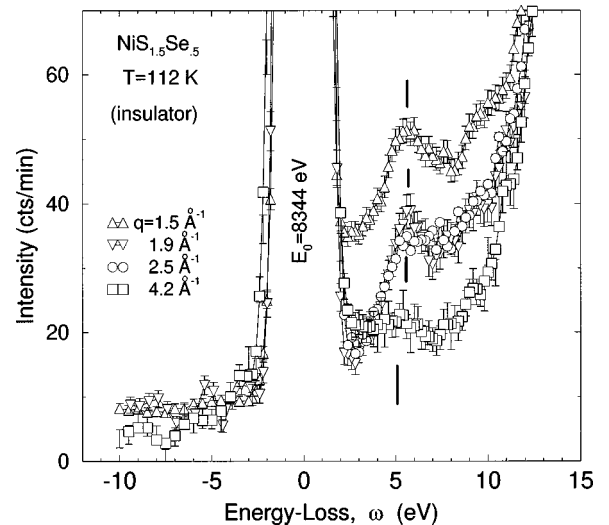


FIG. 8. The q dependence of the charge transfer exciton in $\text{NiS}_{1.5}\text{Se}_{0.5}$.

dramatic, is that over the same momentum-transfer range, the integrated intensity drops by roughly an order of magnitude. The peak at 9.5 eV is too weak to make quantitative statements regarding its q dependence, but does seem to decrease in intensity as q increases. The rapid decrease of intensity with q ties these features in the Raman spectrum to the Coulomb shakeup process described in Fig. 4, diagrams I–III. Diagram I, for instance, would give rise to a $1/q^n$ behavior where $2 < n < 4$. The exact value of n will clearly depend on screening effects and on the range of q relative to the screening length. In $\text{NiS}_{1.5}\text{Se}_{0.5}$ it was observed that $n \cong 3$.

We tentatively identify the feature at 5.5 eV with a charge transfer exciton, associated with the complex consisting of Ni^+ and a $(\text{S}/\text{Se})^-\text{Ni}^{++}$. This object in the phenomenology of the Hubbard model, has a energy (electron notation) $\Delta E = \varepsilon_D - \varepsilon_P + U_D - U_P$. Here ε_D and ε_P are the one electron energies and U_D and U_P the Hubbard on site repulsive energies of an added carrier. Zhang *et al.*^{7,24} have analyzed dispersion properties of such excitons for $\text{Sr}_2\text{CuO}_2\text{Cl}_2$. The feature at 9.5 eV we tentatively identify with a transition from a S/Se $pp\sigma$ or π bonding orbital to an unoccupied S/Se $pp\sigma^*$ antibonding orbital. This peak is not seen in pure NiS_2 possibly due to the fact that the splitting between the S bonding and antibonding states is larger than for the $\text{Ni}(\text{S}/\text{Se})_2$ and therefore it is lost in the relatively stronger $3d \rightarrow 4p$ excitation.

CONCLUSION

Resonant inelastic x-ray scattering makes it possible to probe electronic excitations of the outer electrons in a broad range of materials previously inaccessible to x rays because

of enhanced cross sections. Relaxed selection rules at finite momentum transfer and the presence of a core hole in the intermediate state can lead to very interesting final states including, for example, the charge-transfer excitations observed in $\text{NiS}_{1.5}\text{Se}_{0.5}$. We have described how the dispersion of such excited states arises in a perturbation expansion of the Coulomb interactions among electrons. That this is the case is made clear with the measurements in $\text{NiS}_{1.5}\text{Se}_{0.5}$, where the dispersion of a charge-transfer-like excitation is observed and the spectral weight of that excitation decreases strongly with increasing q . Such a decrease is consistent with the Coulomb coupling picture.

We have stressed the fact, that independent of complex many-body interactions, that if there is one photon in and one photon out, whether on or off resonance, the many-body system being probed is left in an excited state with momentum q and energy ω . This leads us to the conclusion that the width of the features observed in the elastic spectrum are independent of the effects that lead to the core hole lifetime Γ . We predict that the spectral width of any excitation such as a plasmon or an exciton at a band edge in a semiconductor, for instance, will be determined only by its own decay time and not the core hole lifetime.

ACKNOWLEDGMENTS

The authors would like to thank Fu-Chun Zhang for many interesting discussions about excitons in transition-metal compounds. We also thank D. R. Hamann for making his LDA atomic wave function program available to us and for a discussion of momentum conservation and core hole band widths. Thanks is also due to Chi-Chang Kao and Clem Burns for informative discussions of his inelastic Raman data and for his help at beamline X-21 at the NSLS.

-
- ¹E. D. Isaacs and P. M. Platzman, *Phys. Today* **49** (2), 40 (1996).
²C. J. Sparks, Jr., *Phys. Rev. Lett.* **33**, 262 (1974); P. Eisenberger, P. M. Platzman, and J. Winick, *Phys. Rev. B* **13**, 2377 (1976); K. Hamalainen *et al.*, *Phys. Rev. Lett.* **67**, 2850 (1991); C.-C. Kao, W. Caliebe, J. B. Hastings, and J. M. Gillet, *Phys. Rev. B* **54**, 23 (1996); **54**, 16 361 (1996).
³D. Gibbs, D. R. Harshman, E. D. Isaacs, D. B. McWhan, D. Mills, and C. Vettier, *Phys. Rev. Lett.* **61**, 1241 (1988); E. D. Isaacs, P. Zschack, C. L. Broholm, C. Burns, G. Aeppli, A. P. Ramirez, T. T. M. Palstra, R. W. Erwin, N. Stucheli, and E. Bucher, *ibid.* **75**, 1178 (1995).
⁴R. Liu, D. Salamon, M. V. Klein, S. L. Cooper, W. C. Lee, S.-W. Cheong, and D. M. Ginsberg, *Phys. Rev. Lett.* **71**, 3709 (1993).
⁵Y. Y. Wang, F. C. Zhang, V. P. Dravid, K. K. Ng, M. V. Klein, S. E. Schnatterly, and L. L. Miller, *Phys. Rev. Lett.* **77**, 1809 (1996).
⁶J. A. Wilson, in the *Metallic and Non-metallic States of Matter*, edited by P. P. Edwards and C. N. R. Rao (Taylor and Francis, London, 1985), Chap. 9, p. 215.
⁷T. Thio and J. W. Bennett, *Phys. Rev. B* **50**, 10 574 (1994).
⁸P. M. Platzman and P. A. Wolff, *Waves and Interactions in Solid State Plasmas* (Academic, New York, 1973).
⁹P. Nozieres and E. Abrahams, *Phys. Rev. B* **10**, 3099 (1974).
¹⁰M. van Veenendaal, P. Carra, and B. T. Thole, *Phys. Rev. B* **54**, 16 010 (1996).
¹¹P. M. Platzman and N. Tzoar, *Phys. Rev.* **182**, 510 (1969).
¹²F. Sette, G. Ruocco, M. Krisch, U. Bergmann, C. Masciovecchio, V. Mazzacurati, G. Signorelli, and R. Veberni, *Phys. Rev. Lett.* **75**, 850 (1995).
¹³W. Schulke *et al.*, *Phys. Rev. B* **33**, 6744 (1986).
¹⁴F. M. F. de Groot, *Phys. Rev. B* **53**, 7099 (1996).
¹⁵D. R. Hamann (private communication).
¹⁶J. A. Carlisle *et al.*, *Phys. Rev. Lett.* **74**, 1234 (1995).
¹⁷U. Fano, *Phys. Rev.* **104**, 1866 (1961).
¹⁸P. M. Platzman and N. Tzoar (unpublished).
¹⁹P. M. Platzman and Song He, *Phys. Scr.* **T66**, 167 (1996); A. Pinczuk *et al.*, *Phys. Rev. Lett.* **70**, 3983 (1993).
²⁰J. C. W. Folmer *et al.*, *J. Solid State Chem.* **72**, 137 (1988).
²¹A. Bocquet *et al.*, *Phys. Rev. B* **46**, 3771 (1992).
²²A. Y. Matsuura, Z.-X. Shen, D. S. Dessau, C.-H. Park, T. Thio, J. W. Bennett, and O. Jepsen, *Phys. Rev. B* **53**, 7584 (1996).
²³C. A. Burns, E. D. Isaacs, P. Abbamonte, Z. Hasan, T. Thio, and J. W. Bennett (unpublished).
²⁴F. Zhang (unpublished).